Neutron occupancy of the 0d5/2 orbital and the N = 16 shell closure in 24O

K. Tshoo, Y. Satou, C.A. Bertulani, H. Bhang, S. Choi, T. Nakamura, Y. Kondo, S. Deguchi, Y. Kawada, Y. Nakayama, et al.

HAL Id: in2p3-01090228
https://hal.in2p3.fr/in2p3-01090228

Submitted on 12 Jun 2015

Neutron occupancy of the $0d_{5/2}$ orbital and the $N = 16$ shell closure in ^{24}O

K. Tshoo [a,*], Y. Satou [b], C.A. Bertulani [c], H. Bhang [b], S. Choi [b], T. Nakamura [d], Y. Kondo [d],
S. Deguchi [d], Y. Kawada [d], Y. Nakayama [d], K.N. Tanaka [d], N. Tanaka [d], Y. Togano [d],
N. Kobayashi [e], N. Aoi [f], M. Ishihara [g], T. Motobayashi [g], H. Otsu [g], H. Sakurai [g], S. Takeuchi [g],
K. Yoneda [g], F. Delaunay [h], J. Gibelin [h], F.M. Marqués [h], N.A. Orr [h], T. Honda [i], T. Kobayashi [j],
T. Sumikama [j], Y. Miyashita [k], K. Yoshinaga [k], M. Matsushita [l], S. Shimoura [l], D. Sohler [m],
J.W. Hwang [b], T. Zheng [n], Z.H. Li [n], Z.X. Cao [n]

[a] Rare Isotope Science Project, Institute for Basic Science, Daejeon 305-811, Republic of Korea
[b] Department of Physics and Astronomy, Seoul National University, Seoul 151-742, Republic of Korea
[c] Texas A & M University-Commerce, PO Box 3011, Commerce, Texas 75429, USA
[d] Department of Physics, Tokyo Institute of Technology, Tokyo 152-8551, Japan
[e] Department of Physics, University of Tokyo, Tokyo 113-0033, Japan
[f] Research Center for Nuclear Physics, Osaka University, Osaka 567-0047, Japan
[g] RIKEN Nishina Center, Saitama 351-0198, Japan
[h] LPC-Caen, ENSICAEN, Université de Caen, CNRS/IN2P3, 14050 Caen cedex, France
[i] Department of Physics, Rikkyo University, Tokyo 171-8501, Japan
[j] Department of Physics, Tohoku University, Miyagi 980-8578, Japan
[k] Department of Physics, Tokyo University of Science, Chiba 278-8510, Japan
[l] Center for Nuclear Study, University of Tokyo, Saitama 351-0198, Japan
[m] Institute for Nuclear Research of the Hungarian Academy of Sciences, PO Box 51, H-4001 Debrecen, Hungary
[n] School of Physics and State Key Laboratory of Nuclear Physics and Technology, Peking University, Beijing 100871, China

A R T I C L E I N F O

A B S T R A C T

One-neutron knockout from ^{24}O leading to the first excited state in ^{23}O has been measured for a proton target at a beam energy of 62 MeV/nucleon. The decay energy spectrum of the neutron unbound state of ^{23}O was reconstructed from the measured four momenta of the ^{22}O fragment and emitted neutron. A sharp peak was found at $E_{decay} = 50 \pm 3$ keV, corresponding to an excited state in ^{23}O at 2.78 ± 0.11 MeV, as observed in previous measurements. The longitudinal momentum distribution for this state was consistent with d-wave neutron knockout, providing support for a J^{π} assignment of $5/2^{+}$. The associated spectroscopic factor was deduced to be $C^{2}S(0d_{5/2}) = 4.1 \pm 0.4$ by comparing the measured cross section ($\sigma_{-1n}^{exp} = 61 \pm 6$ mb) with a distorted wave impulse approximation calculation. Such a large occupancy for the neutron $0d_{5/2}$ orbital is in line with the $N = 16$ shell closure in ^{24}O.

The neutron drip-line nucleus ^{24}O, which has been studied extensively in recent years [1–14], is now considered a doubly-closed-shell nucleus. In particular, the high excitation energy of the first 2^{+} state [7] and small quadrupole transition parameter [14] are strong indicators of an $N = 16$ spherical shell closure. In addition, Kanungo et al. [8] found a large spectroscopic factor –

$C^{2}S(1s_{1/2}) = 1.74 \pm 0.19$ – for one-neutron knockout from ^{24}O reflecting an almost complete occupancy of the $1s_{1/2}$ orbital.

In this Letter we report on the spectroscopic factor for $d_{5/2}$ neutron removal from ^{24}O. The first excited state of ^{23}O, which is neutron unbound [15,13,16], was populated by one-neutron knockout from ^{24}O with a proton target. The excitation energy, cross section, and longitudinal momentum distribution were determined and allowed the $0d_{5/2}$ neutron-hole nature of this state to be identified. The large spectroscopic factor deduced for this state is in line with the $N = 16$ shell closure in ^{24}O.

* Corresponding author.
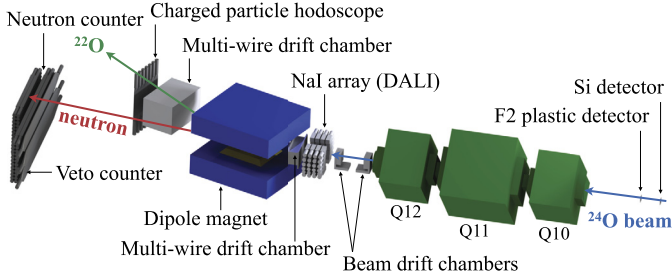E-mail address: tshoo@ibs.re.kr (K. Tshoo).

Fig. 1. (Color online.) Schematic view of the experimental setup.

The experiment was performed at the RIPS facility [17] at RIKEN. The experimental setup has been described in Refs. [14,18], and is depicted in Fig. 1. The secondary ^{24}O beam was produced using a 1.5 mm-thick Be production target and a 95 MeV/nucleon ^{40}Ar primary beam of $\sim$40 pnA. The average intensity of the ^{24}O beam was $\sim$4 particles/sec. The momentum of the secondary beam was determined particle-by-particle by measuring the position at the dispersive focus F1 of RIPS with a parallel plate avalanche counter. The energy loss (ΔE) and time-of-flight (TOF) were measured using 350 µm-thick silicon and 500 µm-thick plastic scintillator detectors, respectively, at the achromatic focus F2. The liquid-hydrogen (LH$_2$) target [19] was installed at the achromatic focus F3. The effective target thickness and the mid-target energy of ^{24}O were 159 ± 3 mg/cm^2 and 62 MeV/nucleon, respectively. The ^{24}O beam incident on the target was tracked particle-by-particle by using two multi-wire drift chambers installed just upstream of the target. The target was surrounded by an array consisting of 48 NaI(Tl) crystals (DALI) to detect γ rays from de-excitation of the fragments.

The $B\rho$-TOF-ΔE method was employed to determine mass and charge of the fragment following reactions of the ^{24}O beam with the LH$_2$ target. The magnetic rigidity ($B\rho$) was determined from the position and angle information measured with two multi-wire drift chambers placed at the entrance and exit of the dipole magnet. The TOF of the fragment was measured with the plastic scintillator charged particle hodoscope which also gave energy loss information. The beam velocity decay neutron was detected using a plastic scintillator counter array placed some 4.7 m downstream of the target, equipped with a charged particle veto counter. A neutron detection efficiency of $25 \pm 1\%$ at 64 MeV was measured for a 2 MeVee threshold in a separate ^{7}Li(p, n) measurement performed during the experiment.

The decay energy spectrum of ^{23}O* was reconstructed from the measured four momenta of ^{22}O and the emitted neutron. The decay energy E_{decay} is expressed as:

$$E_{\text{decay}} = \sqrt{(E_f + E_n)^2 - |\boldsymbol{p}_f + \boldsymbol{p}_n|^2} - (M_f + M_n), \qquad (1)$$

where $E_f(E_n)$, $\boldsymbol{p}_f(\boldsymbol{p}_n)$, and $M_f(M_n)$ are the total energy, momentum, and mass of ^{22}O (neutron), respectively. Fig. 2 shows the decay energy spectrum in terms of cross section (dσ/dE_{decay}) after correcting for the detection efficiencies and acceptances. The background contribution was subtracted here by using data taken with an empty target. The error bars are statistical only. The geometrical acceptance was estimated using a Monte Carlo simulation taking into account the beam profile, geometry of the setup, experimental resolutions, and multiple scattering of the charged particles. The experimental energy resolution was estimated to be $\Delta E_{\text{decay}} \approx 0.52\sqrt{E_{\text{decay}}}$ (MeV) in FWHM.

The decay energy spectrum was described using one resonance for the peak at $E_{\text{decay}} = 50 \pm 3$ keV and a Maxwellian distribution for the non-resonant continuum [20]. The peak observed has an
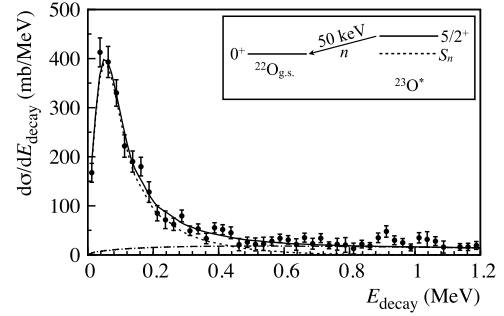

Fig. 2. The cross section, dσ/dE_{decay}, obtained by measuring a neutron in coincidence with ^{22}O. The error bars are statistical only. The dotted and dot-dashed lines are the results of the fits for a resonance at $E_{\text{decay}} = 50 \pm 3$ keV and a non-resonant continuum component [20], respectively. The decay path from the first excited state of ^{23}O to the ground state of ^{22}O is represented in the inset.

Table 1
The excitation energies of the first two states in ^{23}O and the spectroscopic factors for neutron removal from ^{24}O are compared with the results of the USDB and WBT shell-model calculations.

J^π	Energy (MeV)			Spectroscopic factor C^2S		
	Exp.	USDB	WBT	Exp.	USDB	WBT
$1/2^+$	0.0	0.0	0.0	1.74 ± 0.19[a]	1.81	1.73
$5/2^+$	2.78 ± 0.11	2.59	2.72	4.1 ± 0.4	5.67	5.52

[a] From Ref. [8].

asymmetric lineshape owing to its proximity to threshold, and its width is fully dominated by the experimental resolution. The corresponding excitation energy is $E_x = 2.78 \pm 0.11$ MeV, given the separation energy of $S_n(^{23}$O$) = 2.73 \pm 0.11$ MeV [21–23]. Since no γ-ray lines were observed for the ^{22}O$-n$ channel, we assumed that ^{22}O is in the ground state. As such, the location of the resonance is in good agreement with previous experiments [15,16].

The one-neutron knockout cross section to the resonance at $E_{\text{decay}} = 50$ keV was determined to be $\sigma_{-1n}^{\text{exp}} = 61 \pm 6$ mb, after subtracting the non-resonant continuum. The quoted error arises from the uncertainty in the choice of the functional form describing the non-resonant continuum (8%), statistical uncertainty (4%), neutron detection efficiency (3%), and the target thickness (2%).

The single-particle configurations for the ground states of ^{23,24}O are expected to be $\nu(0d_{5/2})^6\nu(1s_{1/2})^1$ and $\nu(0d_{5/2})^6\nu(1s_{1/2})^2$, respectively, in the shell-model picture (see, e.g., Refs. [8,24]), and suggest that the first excited state of ^{23}O presented here (neutron hole state) is very likely to be populated by the $0d_{5/2}$ neutron knockout. Calculations using the USDB interaction [25] in the *sd* model space, as well as WBT [26] interaction in the *spsdpf* model space, predict that the spin-parity of this state is $J^\pi = 5/2^+$ (Table 1).

The one-neutron knockout cross section, above a few tens MeV/nucleon energy, can be decomposed into the single-particle cross section (σ_{sp}) related to the reaction and the spectroscopic factor (C^2S) reflecting the nucleon occupancy [27], as follows:

$$\sigma_{-1n} = \sum_{nlj} \left(\frac{A}{A-1}\right)^\Lambda C^2S\left(J^\pi, nlj\right)\sigma_{\text{sp}}(nlj, S_n^{\text{eff}}), \qquad (2)$$

where J^π is the spin-parity of the final state of the residue (core); nls denote the quantum numbers of the knocked-out neutron; S_n^{eff} is the effective separation energy which corresponds the sum of the neutron separation energy of the projectile and the excitation energy of the core; A is the mass number of the projectile; $(A/(A-1))^\Lambda$ is the center-of-mass correction factor [28] where A is the mass number of the projectile and Λ is the major oscillator quantum number given by the relation of $\Lambda = 2n + l$.
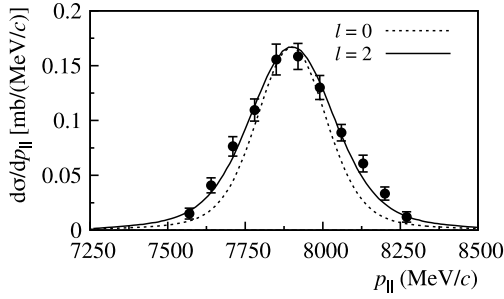
Fig. 3. Longitudinal momentum distribution for ^{23}O* (see text). The error bars are statistical only. The solid and dashed lines represent the calculated longitudinal momentum distributions normalized to the peak of the measured distribution for the knockout of neutrons in the $0d_{5/2}$ and $1s_{1/2}$ orbitals, respectively. The distributions were convoluted with the experimental resolution.

The single-particle cross section assuming a spectroscopic factor of unity was calculated using the distorted wave impulse approximation (DWIA) calculation for the quasifree (p, pn) reaction as described in Ref. [29]. The calculation employed the eikonal approximation for the distorted wave functions of incoming and outgoing reaction channels. The effective nucleon–nucleon interaction M3Y [30] along with the Coulomb potential was adopted for the real part of the optical potential. The nucleon–nucleus cross section in nuclear matter developed in Refs. [31–33] and the densities of the projectile, or core, folded with the matter density of proton were employed to introduce the imaginary part of the optical potential.

The wave functions of single-particle neutron orbits around the core were calculated using the Woods–Saxon potential in the manner as described in Ref. [34]. The Skyrme (SkX) Hartree–Fock (HF) calculation [35] was employed to deduce the root-mean-squared (rms) radius r_{HF} of each single-particle orbit in the projectile. The code NUSHELL [36] was used for this calculation. The HF rms radius of ^{24}O was $r_{HF} = 3.434$ fm for the $0d_{5/2}$ orbital. The reduced radius r_0 was determined so that the calculated single-particle wave function within the potential well adopting a diffuseness of $a_0 = 0.7$ fm satisfies $r_{sp} = \sqrt{A/(A-1)}r_{HF}$ at the HF predicted binding energy. The reduced radius was calculated to be 1.171 fm for the $0d_{5/2}$ orbital. With this r_0, the depth of the potential well was further adjusted to reproduce S_n^{eff}. The S_n^{eff} was calculated for the 2.78-MeV state to be 6.97 MeV by adopting $S_n(^{24}$O$) = 4.19 \pm 0.14$ MeV [21].

The single-particle cross section was calculated to be $\sigma_{sp} = 13.5$ mb, from which we deduced the spectroscopic factor $C^2S^{exp}(0d_{5/2}) = 4.1 \pm 0.4$ by using Eq. (2). The one-neutron knockout cross section was calculated to be $\sigma_{-1n}^{th}(0d_{5/2}) = 83.1$ mb by employing the shell-model spectroscopic factor of $C^2S^{th} = 5.67$ obtained using the USDB interaction. The reduction factor defined as $R_s = \sigma_{-1n}^{exp}/\sigma_{-1n}^{th}$ was derived to be $R_s = 0.73 \pm 0.07$ which is consistent with the systematics in Refs. [37,34]. Moreover, a reduction factor of $R_s = 0.84 \pm 0.10$ may be deduced for inclusive one-neutron knockout at 51 MeV/nucleon from the neighboring $N = 14$ closed sub-shell nucleus ^{22}O [38].

In the core $(^{23}$O$) + n$ system description, the width of the longitudinal momentum $(p_\parallel)$ distribution of the core is directly linked to the single-particle wave function of the knocked-out neutron, and can be utilized to identify its orbital angular momentum (l). We have reconstructed here the longitudinal momentum distribution of ^{23}O* from the measured momenta of the ^{22}O fragment and neutron.

The $p_\parallel$ distribution for the first excited state of ^{23}O in the laboratory frame is displayed in Fig. 3. The error bars are statistical only. The width of the distribution was determined to be 356 ± 28 MeV/c (FWHM) by a Gaussian fit. The experimental dis-
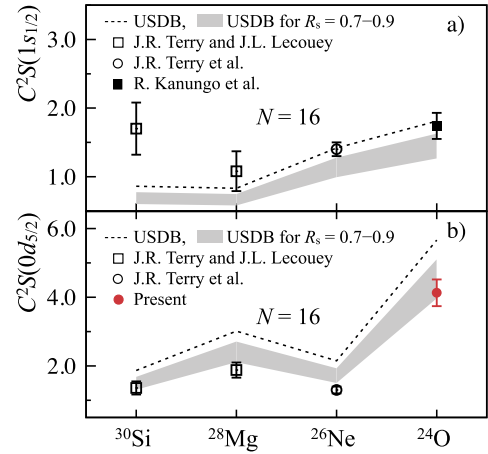
Fig. 4. (Color online.) Spectroscopic factors of the lowest $1/2^+$ and $5/2^+$ states, $C^2S(1s_{1/2})$ (a) and $C^2S(0d_{5/2})$ (b), in even–even $N = 16$ isotones. The experimentally determined spectroscopic factors (data points) taken from Refs. [8,40,41] were derived from the neutron knockout reactions on a beryllium target. The present result is shown by the red-filled circle. The results of the USDB shell-model calculation are represented by the dashed lines. The gray bands indicate the results of the calculations including a reduction factor R_s, where the upper and lower limits of the bands correspond to 0.9 and 0.7, respectively.

tribution is compared in Fig. 3 with the DWIA calculations. The results of the calculation for the removal of $0d_{5/2}$ (solid line) and $1s_{1/2}$ (dashed line) neutrons are shown in Fig. 3, where the calculated distributions were convoluted with the momentum resolution. The momentum resolution was determined to be 195 MeV/c (FWHM) using the Monte Carlo simulation taking into account the momentum spread of the ^{24}O beam, range difference of incoming and outgoing particles inside the LH$_2$ target, Coulomb multiple scattering effects, and the detector resolutions. The widths of the calculated distributions for the $0d_{5/2}$ and $1s_{1/2}$ knocked-out neutrons were to be 334 and 270 MeV/c (FWHM), respectively. The result for $0d_{5/2}$ neutron knockout reproduces well the momentum distribution, supporting the spin-parity assignment of $J^\pi = 5/2^+$. It should be noted that this state has also been measured via two-proton and one-neutron removal [15] and proton inelastic scattering [16].

The excitation energy and the spectroscopic factor for neutron removal from ^{24}O are compared with the results of the shell-model calculations using the USDB and WBT interactions in Table 1. Both calculations reproduce the energy and also the spectroscopic factor assuming a reduction factor of $R_s \approx 0.7$–0.9 suggested by Gade et al. [37,34]. We note that the USDB interaction successfully describes the energies of the first excited states and the quadrupole transition parameters of ^{22,24}O reported in Refs. [14,39].

Fig. 4 shows the proton number dependency of the experimentally determined and calculated (dashed lines) spectroscopic factors for the even–even $N = 16$ isotones. While the spectroscopic factor for the $\nu 1s_{1/2}$ orbital gradually increases in moving from $Z = 12$ to 8, that for the $\nu 0d_{5/2}$ orbital dramatically rises at $Z = 8$. This trend is reasonably well reproduced by the USDB shell model calculations. Significantly, the $C^2S(0d_{5/2})$ for ^{24}O is much larger than those of other isotones, indicating a large neutron occupancy of the $0d_{5/2}$ orbital. These results are in line with an $N = 16$ sub-shell closure in ^{24}O.

The gray bands in Fig. 4 represent the results of the USDB shell-model calculations including a reduction factor of $R_s = 0.7$–0.9. As such, the experimentally determined spectroscopic factors for the $\nu 0d_{5/2}$ orbit are in agreement with the calculations. While the reduction factor is close to unity for the $1s_{1/2}$ neutron (for $Z \leq 14$), it is smaller than unity for the $0d_{5/2}$ neutron ($R_s \approx 0.7$–0.8). This

behaviour may provide a benchmark to test more sophisticated nuclear structure models, as well as reaction mechanisms. Recently, for example, Grinyer et al. [42] have investigated the quenching of the spectroscopic factors in ^{10}Be and ^{10}C for one-neutron knockout and found that an *ab initio* structure calculation, taking both 3-body forces and continuum effects into account, well describes the reduction.

In summary, we have investigated the occupancy of the neutron $0d_{5/2}$ orbital in ^{24}O via one-neutron knockout from ^{24}O with a proton target. The excitation energy of the first excited state of ^{23}O was measured to be 2.78 ± 0.11 MeV and the spin-parity was assigned, based on the longitudinal momentum distribution, to be $J^{\pi} = 5/2^+$. The large corresponding spectroscopic factor of $C^2 S^{\exp}(0d_{5/2}) = 4.1 \pm 0.4$ supports the picture of an $N = 16$ spherical shell closure in ^{24}O.

Acknowledgements

References

[1] A. Ozawa, et al., Phys. Rev. Lett. 84 (2000) 5493.
[2] R. Kanungo, I. Tanihata, A. Ozawa, Phys. Lett. B 528 (2002) 58.
[3] M. Stanoiu, et al., Phys. Rev. C 69 (2004) 034312.
[4] B.A. Brown, W.A. Richter, Phys. Rev. C 72 (2005) 057301.
[5] A. Volya, V. Zelevinsky, Phys. Rev. Lett. 94 (2005) 052501.
[6] C.R. Hoffman, et al., Phys. Rev. Lett. 100 (2008) 152502.
[7] C.R. Hoffman, et al., Phys. Lett. B 672 (2009) 17.
[8] R. Kanungo, et al., Phys. Rev. Lett. 102 (2009) 152501.
[9] T. Otsuka, et al., Phys. Rev. Lett. 87 (2001) 082502.
[10] T. Otsuka, et al., Phys. Rev. Lett. 95 (2005) 232502.
[11] T. Otsuka, et al., Phys. Rev. Lett. 105 (2010) 032501.
[12] Ø. Jensen, et al., Phys. Rev. C 83 (2011) 021305(R), http://dx.doi.org/10.1103/PhysRevC.83.021305, http://link.aps.org/doi/10.1103/PhysRevC.83.021305.
[13] C.R. Hoffman, et al., Phys. Rev. C 83 (2011) 031303(R), http://dx.doi.org/10.1103/PhysRevC.83.031303, http://link.aps.org/doi/10.1103/PhysRevC.83.031303.
[14] K. Tshoo, et al., Phys. Rev. Lett. 109 (2012) 022501.
[15] A. Schiller, et al., Phys. Rev. Lett. 99 (2007) 112501.
[16] Y. Satou, et al., Few-Body Syst. 54 (2013) 287.
[17] T. Kubo, et al., Nucl. Instrum. Methods B 70 (1992) 309.
[18] Y. Satou, et al., Phys. Lett. B 728 (2014) 462.
[19] H. Ryuto, et al., Nucl. Instrum. Methods A 555 (2005) 1.
[20] F. Deák, et al., Nucl. Instrum. Methods A 258 (1987) 67.
[21] M. Wang, et al., Chin. Phys. C 36 (2012) 1603.
[22] B. Jurado, et al., Phys. Lett. B 649 (2007) 43.
[23] N.A. Orr, et al., Phys. Lett. B 258 (1991) 29.
[24] D. Cortina-Gil, et al., Phys. Rev. Lett. 93 (2004) 062501.
[25] B.A. Brown, W.A. Richter, Phys. Rev. C 74 (2006) 034315.
[26] E.K. Warburton, B.A. Brown, Phys. Rev. C 46 (1992) 923.
[27] P.G. Hansen, J.A. Tostevin, Annu. Rev. Nucl. Part. Sci. 53 (2003) 219.
[28] A.E.L. Dieperink, T. de Forest, Phys. Rev. C 10 (1974) 543.
[29] T. Aumann, C.A. Bertulani, J. Ryckebusch, Phys. Rev. C 88 (2013) 064610.
[30] G. Bertsch, et al., Nucl. Phys. A 284 (1977) 399.
[31] C.A. Bertulani, C. De Conti, Phys. Rev. C 81 (2010) 064603.
[32] E. Clementel, C. Villi, Il Nuovo Cimento 2 (1955) 176.
[33] C.A. Bertulani, Braz. J. Phys. 16 (1986) 380.
[34] A. Gade, et al., Phys. Rev. C 77 (2008) 044306.
[35] B.A. Brown, Phys. Rev. C 58 (1998) 220.
[36] B.A. Brown, W.D.M. Rae, MSU-NSCL report, 2007.
[37] A. Gade, et al., Phys. Rev. Lett. 93 (2004) 042501.
[38] E. Sauvan, et al., Phys. Rev. C 69 (2004) 044603.
[39] E. Becheva, et al., Phys. Rev. Lett. 96 (2006) 012501.
[40] J.R. Terry, J.L. Lecouey, Nucl. Phys. A 734 (2004) 469.
[41] J.R. Terry, et al., Phys. Lett. B 640 (2006) 86.
[42] G.F. Grinyer, et al., Phys. Rev. Lett. 106 (2011) 162502.